Elucidating the dynamical equilibrium of C_{60} molecules on Ag(111)

K. Pussi, H. I. Li, Heekeun Shin, L. N. Serkovic Loli, A. K. Shukla, J. Ledieu, V. Fournée, L. L. Wang, S. Y. Su, K. E. Marino, M. V. Snyder, and R. D. Diehl

Phys. Rev. B **86**, 205406 — Published 5 November 2012

DOI: 10.1103/PhysRevB.86.205406

Elucidating the dynamical equilibrium of C_{60} molecules on Ag(111)

K. Pussi[1], H. I. Li[2], Heekeun Shin[2], L. N. Serkovic Loli[3], A. K. Shukla[3], J. Ledieu[3], V. Fournée[3], L. L. Wang[4], S. Y. Su[2], K. E. Marino[2], M. V. Snyder[2], and R. D. Diehl[2]

[1]*Department of Mathematics and Physics, Lappeenranta University of Technology, P.O. Box 20 FIN-53851 Lappeenranta, Finland*

[2]*Department of Physics, Penn State University, University Park, PA 16802*

[3]*Institut Jean Lamour, UMR 7198 CNRS-Nancy Université-UPV Metz, 54042 Nancy, France*

[4]*Division of Materials Science & Engineering, Ames Laboratory, Ames, IA 50011*

Abstract

We have used scanning tunneling microscopy, low-energy electron diffraction and density functional theory to elucidate the structure and thermodynamics of the $(2\sqrt{3}x2\sqrt{3})R30°$ phase of C_{60} on Ag(111), which consists of a mixture of molecules in two different site/orientation states. The structure analysis identifies the two types of molecules as (1) sitting on a vacancy with a hexagon face down and (2) sitting on a top site with a C-C bond down. The molecules flip between the two states at a temperature-dependent rate. We show using a thermodynamic analysis that the two states differ by 0.07 eV and are separated by an energy barrier of 0.84 eV. Their dynamical equilibrium involves the diffusion of surface vacancies between C_{60} molecules, producing spatially and temporally correlated flipping events.

PACS Numbers: 68.35.bp, 68.43.De, 68.43.Fg, 61.05.jh

The use of molecules as active components in electronic circuits is a well-established goal [1], and C_{60} serves as a prototypical molecule for such applications. It is well known that the conductance through C_{60} molecules on surfaces to an external electrode is strongly dependent on their orientation on the surface [2-6], the surface adsorption site [7] and their density [8]. Although molecular adsorption geometry may be fixed by strong covalent bonds on some substrates [9-11], other surfaces present more variable interfaces [12-15], which raises the possibility of controlling the conductance. However, identifying their adsorption geometries and understanding how they vary have been challenging.

Earlier STM studies established that the equilibrium structure for an annealed C_{60} monolayer on Ag(111) consists of a randomly mixed phase of "bright" and "dim" molecules in a $(2\sqrt{3}x2\sqrt{3})R30°$ commensurate superstructure and that at room temperature, the molecules flip between the two states [16, 17]. High-resolution STM images at low temperatures identified the dim molecules as being oriented with a hexagon down (hex), and bright molecules as oriented with a 6:6 C-C bond down (6:6) [18]. A similar situation was observed for C_{60} on Au(111) [4], and in that case, it was suggested recently [19, 20] that the bright and dim molecules might also correspond to C_{60} in different adsorption sites. In particular, it was proposed that the dim molecules reside in "nano-pits" or vacancies, while the bright molecules remain on top of the surface. A similar but more complex flipping situation also has been observed for C_{60} on Ag(100) [21].

The formation of such "nano-pits" is now viewed to be a fairly common occurrence for C_{60} on certain close-packed metal surfaces [9, 10, 22-24] and has been suggested to arise from the Coulomb repulsion between the ionically-bound molecules [25]. The nature of these nano-pits for C_{60} on Ag(111) were revealed in our recent low-temperature LEED study to consist of single-atom vacancies [26]. The adsorption geometry of the bright molecules, however, was not determined. We show here, using a combination of STM, LEED and DFT, that the hex and 6:6 molecules on Ag(111) adsorb in vacancy and top sites, respectively, and that the "flipping" activity observed in STM consists of a concerted motion of a substrate vacancy and a rotation of the C_{60}. We also present the first quantitative study of the temperature dependence of such flipping. From the measurements of the kinetics of this flipping, we have deduced the activation energy for the flipping to be 0.84 eV on Ag(111), with an energy difference between the two states of 0.07 eV. In this paper, we present the quantitative determination of the geometries of the bright and dim

molecules, a model for their dynamical equilibrium, and some insight into the flipping and its relationship to vacancy diffusion.

The studies described here were performed on the commensurate Ag(111)-(2√3x2√3)R30°-C_{60} structure, which was prepared by dosing the surface with C_{60} at room temperature and annealing for several minutes at 400°C. After dosing, the C_{60} monolayer consists of a mixture of several different phases, most of them incommensurate [13, 16], but annealing results in a monolayer that is almost exclusively the (2√3x2√3)R30° structure and consists of the bright and dim molecules discussed earlier. By studying the dynamics of the bright-dim C_{60} flipping on Ag(111) using an Omicron variable-temperature STM in the temperature range of 280 K to 330 K, we discovered four things. First, the flipping rate from bright to dim is the same as from dim to bright, indicating an equilibrium situation. Second, the flipping rate is temperature dependent. Third, flips from bright to dim are correlated to nearby flips from dim to bright, and fourth, the ratio of the numbers of bright and dim depends on temperature.

Figures 1a and 1b show STM images at 295 K and 333 K, respectively, indicating that most of the molecules are in either bright or dim states. There are also three molecules in Fig. 1a and one in Fig 1b that are in a state that we call "superbright", a minority species comprising 1-3% of the molecules and which we believe is related to surface strain. In this work, we are concerned with the flipping between the bright and dim states. The insets show difference images of two successive STM images, separated in time by 43 s. A dark "hole" indicates that a molecule has flipped from bright to dim, and a bright spot indicates that a molecule has flipped from dim to bright.

The flipping rates for both types of flips (bright to dim and dim to bright) are shown in **Figure 1c**. At any given temperature, the two flipping rates are essentially identical, indicating an equilibrium situation. Assuming an exponential dependence, we deduced the flip activation energy to be 0.84 ± 0.05 eV, with a prefactor of $5 \pm 1 \times 10^{10}$ s^{-1}. The temperature range we used here was limited by the scanning speed of the STM and the kinetics of the flipping. At lower temperatures, the flipping was so slow that the equilibration time was hours or more, and at higher temperatures, multiple flips would occur between frames, making it impossible to measure the flipping rate.

The temperature dependence of the ratio of bright to dim molecules for C_{60} on Ag(111) is plotted in **Figure 1d**. The ratio of bright to dim decreases as the temperature is increased, consistent with the dim being the more stable configuration. Therefore, a simple picture of the equilibrium is of two states having different energies and separated by a large energy barrier, as shown in **Figure 1e.** Assuming an exponential dependence for the bright-dim ratio, we have deduced that the energy difference between the two states is 0.07 ± 0.02 eV.

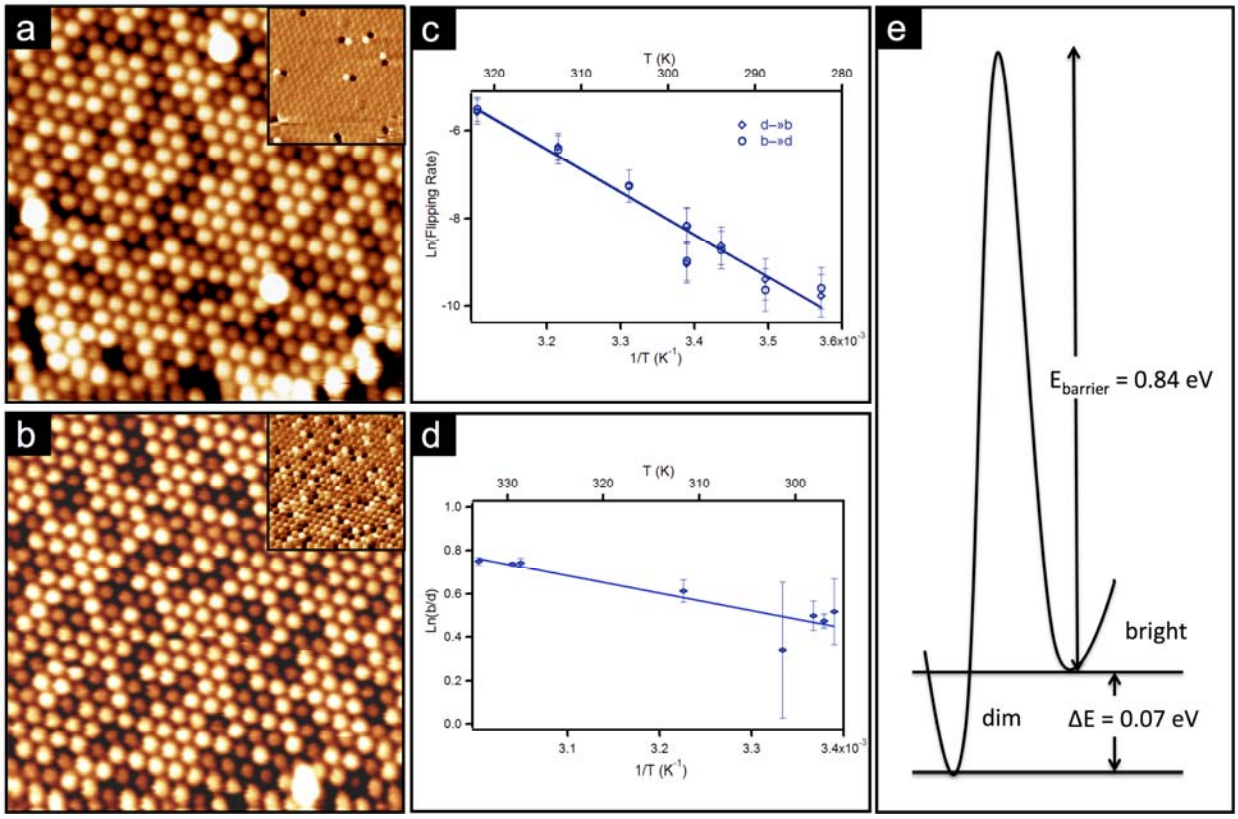

Figure 1 (color online) (a) 20 x 20 nm^2 STM image of Ag(111)-(2√3x2√3)-C_{60} at T = 295 K and tunneling parameters I = 0.06 nA, V= +1.2 V. Inset: Difference between the image shown and the previous one, 43 s earlier. (b) 20 x 20 nm^2 STM image of same surface at T = 333 K and I = 0.07 nA, V= +2.2 V. The inset showing the difference of two successive frames (43 s apart) demonstrates more rapid flipping at the higher temperature. (c) Rate of flipping from bright to dim and dim to bright, as a function of inverse temperature. The slope of the graph indicates an activation energy of 0.84 ± 0.05 eV. (d) Bright/dim ratio vs. inverse T for C_{60} on Ag(111) indicating an energy difference of 0.07 ± 0.02 eV. (e) Schematic diagram of a 2-state model for the bright and dim molecules.

It is evident in **Figures 1a and 1b** that most of the bright-dim flips involve adjacent C_{60} molecules. In order to understand this process better, we have carried out a structural analysis to obtain the geometrical details of the C_{60} molecules. This includes a new analysis of the LEED intensities at T = 32 K for Ag(111)-(2√3x2√3)R30°-C_{60}. The measurement and calculation methods were described in an earlier paper [26]. In that work, it was assumed that at T = 32 K, only one species of C_{60} would be present, but our subsequent STM measurements as low as T = 50 K indicated that this is not the case, because the flipping kinetics are too slow for the monolayer to reach equilibrium. In the analysis presented here, the diffraction intensities were treated as an incoherent sum of diffraction from the two types of C_{60} due to the randomness of the spatial distribution, and the ratio was varied to obtain the optimum fit. To reduce the computational burden of testing all possible configurations, we limited the test models to those that are consistent with the high-resolution STM images [18]. In order to limit the number of parameters to be fitted, only the coordinates perpendicular to the surface were allowed to vary in the optimization. While there are undoubtedly some lateral relaxations in this structure, LEED generally is not very sensitive to them and any such parameters determined would have low precisions. Our aim here is to pinpoint the structural features that give rise to the bright-dim contrast in the STM images.

Figure 2 shows the molecular orientations considered in the calculations. The hex molecules are aligned with their mirror planes parallel to the mirror plane of the substrate. The 6:6 molecules have a mixture of three symmetrically-equivalent orientations in which the mirror planes of the molecules point toward next-nearest neighbors, or 30° from the substrate mirror planes [26].

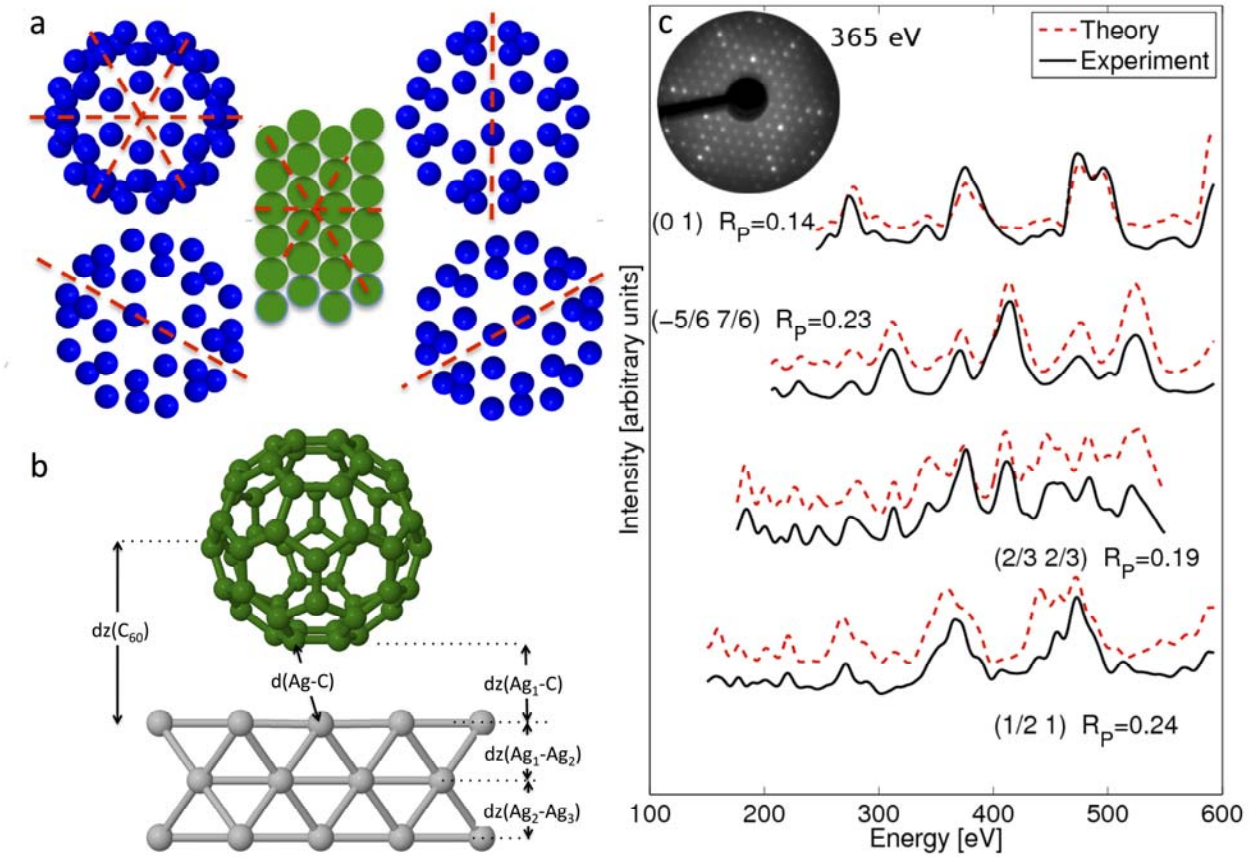

Figure 2. (color online) (a) Orientations of C_{60} molecules found in high-resolution STM studies on Ag(111). The molecular mirror planes are indicated by dashed lines. The center panel shows the orientation of the top substrate layer, having indicated mirror planes. (b) Schematic drawing showing the parameter definitions for Table 1. (c) Representative LEED spectra and LEED pattern for Ag(111)-(2√3x2√3)-R30°-C_{60}. The full set of 15 beams, having a total energy range of 4860 eV, is given in the supplementary material [27].

The calculated spectra were compared to the measured spectra by the Pendry R-factor [28], which has a value 0 for identical spectra and 1 for no correlation. In the first pass through the trial structures (consisting of different site-orientation configurations), all adsorption sites except top and vacancy were ruled out for both substrates by having R-factors greater than 0.7. To distinguish between the remaining models, we note that models yielding R-factors greater than the optimum R-factor + RR (RR = the variance of the Pendry R-factor) can be significantly excluded based on statistical grounds.

After testing the models thus generated, the best R-factors for the different configurations of C_{60} on Ag(111) were in the range of 0.34 – 0.40. After mixing the hex and 6:6 molecules, the R-factors were between 0.24 and 0.28. The RR factor was 0.02; therefore models having R > 0.26 are very unlikely to correspond to the true structure. This allowed us to rule out the 6:6-vac geometry, leaving mixtures of either hex-top or hex-vac molecules with 6:6-top molecules. Since the earlier DFT results indicated that the hex-top is less favorable than the hex-vac by at least 0.3 eV [26], we excluded it from further analysis. As indicated in **Table I**, the best result for T = 32 K is a 50:50 mixture of hex-vac and 6:6-top molecules. Furthermore, the hex molecules comprise a 50:50 mixture of mirror planes parallel and antiparallel to the substrate mirror plane, as found in the earlier study [26], while the C:C bond molecules are equally distributed between the three symmetry-equivalent orientations. The mixed analysis resulted in a significant improvement over the R-factor (0.34) obtained using only hex-vac C_{60}.

Table I. Best Pendry R-factors obtained from the specified mixtures of C_{60} molecules on Ag(111). Hex refers to the hexagon-down orientation, 6:6 refers to the C-C bond down orientation, top or vac refers to the top or vacancy adsorption site respectively, and the angles refer to the orientation of the molecular mirror plane relative to the substrate mirror plane (see **Figure 2**).

C_{60}/Ag(111) Incoherent mixing	Hex top (0° + 180°)	Hex vac (0° + 180°)	6:6 top (30°)	6:6 vac (30°)
Hex top (0° + 180°)	0.35	0.34	0.25	0.28
Hex vac (0° + 180°)	0.34	0.34	**0.24**	0.28
6:6 top (30°)			0.37	
6:6 vacancy (30°)				0.40

Some representative LEED spectra from each case are shown in **Figure 2c**, and the full set of spectra is given in the supplementary material [27]. **Table II** gives some of the structural parameters determined by LEED, according to the schematic drawings shown in **Figures 2b**. Both structures involve a small relaxation of the substrate atoms closest to the C_{60} molecules.

There is very little deformation of the C_{60} molecules, presumably due to the large energy cost to deform the C-C bonds, compared to the C_{60}–Ag bonds.

Table II. Best-fit parameters for C_{60} on Ag(111) according to the LEED analysis. The parameters are defined in Figure 2. d(Ag-C) corresponds to the nearest-neighbor distance between the C_{60} and the Ag; the rest are perpendicular distances. Δ corresponds to the average intralayer buckling amplitude. Dimensions are in Å. The bulk interlayer spacing of Ag(111) is 2.35 Å.

Parameter	**Hex-vac**	**6:6 - top**
dz(C_{60})	5.2 ± 0.1	5.5 ± 0.1
d(Ag-C)	2.5 ± 0.1	2.1 ± 0.1
dz(Ag_1-C)	2.0 ± 0.1	2.0 ± 0.1
dz(Ag_1-Ag_2)	2.35 ± 0.03	2.34 ± 0.04
dz(Ag_2-Ag_3)	2.34 ± 0.04	2.34 ± 0.05
dz(Ag_3-Ag_4)	2.35 ± 0.06	2.34 ± 0.06
Δ_1	0.03 ± 0.03	0.05 ± 0.04
Δ_2	0.02 ± 0.04	0.06 ± 0.05
Δ_3	0.03 ± 0.05	0.05 ± 0.06

Although the mechanism for the formation of the nano-pits under fullerenes has been investigated [10, 24, 25], the dynamics of the bright-dim flipping has not. As shown in Figure 1, the flipping in this case usually involves adjacent C_{60} molecules. We have shown here that the dim molecules are on vacancies and bright molecules are on top sites; therefore the adjacent bright-dim flipping implies that a substrate atom has disappeared from one C_{60} site and appeared at an adjacent C_{60} site, and that most of the energy barrier for the flipping must be the energy cost for a vacancy to move from beneath a C_{60} molecule to an intermediate site. The experimental observation of flipping thus involves the rapid diffusion of substrate vacancies between the C_{60} sites, to which the vacancy is strongly attracted. The diffusion barrier for a vacancy on Ag(111) has been calculated using surface embedded atom method to be 0.404 eV [29], compared to the flipping barrier we have measured of 0.84 eV. The flipping process is more complex however.

When a flip occurs, there are multiple diffusion paths for the vacancy, i.e. if the vacancy jumps from site to site on the Ag(111) surface, then at least four hops are required to move from one C_{60} to the next. That also precludes a direct interpretation of the measured exponential prefactor (5×10^{10} s^{-1}), which is related to the attempt frequency, and which for many simple examples of diffusion can be related to the lateral vibrational frequency of the vacancy [30].

To gain insight into the energetics of this process, we have extended the earlier DFT studies [26, 31] to include 6:6 orientations, and we have also looked at a $(4\sqrt{3}x2\sqrt{3})R30°$ surface supercell that accommodates two C_{60} molecules, in order to explore the effects of mutual C_{60} orientations on their stability. While this model has many shortcomings, e.g. it is not possible to describe the complex distribution of C_{60}'s with just two molecules, it does provide some useful insight, as described below. In order to achieve a convergence with an error below 0.01 eV for the adsorption energy, it was necessary to increase the k-point mesh in this calculation from (3x3x1) mesh used earlier [26, 31] to (6x6x1). This shifts the absolute values of the adsorption energies somewhat, but the relative differences between configurations are maintained.

Table III indicates the adsorption energy per C_{60} molecule for various configurations, referenced to an isolated monolayer of hex-orientation C_{60}. Using this reference means that the average C_{60}-C_{60} interaction energy is mostly excluded from the adsorption energies, but orientational effects will remain. In cases where a vacancy is formed, the exact location of the extracted substrate atom has a significant effect on the adsorption energy. We have calculated the energies for two limits. In the first, the Ag atom is allowed to adsorb on top of the surface (denoted as "*rec*" in our previous work). In the second, the Ag atom takes a lattice site in the bulk of the crystal. The true situation is likely to be within this range. The values in **Table III** indicate that with only one type of C_{60} molecule present, the hex-vac geometry is much more favorable than the hex-top, while the 6:6-top is more favorable than the 6:6-vac. The preference for hex-vac extends to the mixed system, with the most favorable situation having all molecules in hex-vac geometries, and the second-most favorable situation hex-vac + 6:6-top. The ordering of the adsorption energies for the 2-C_{60} case is the same as for the 1-C_{60} case, suggesting that the mutual molecular orientation of neighbors does not strongly affect the adsorption energies. These results, along with the dependence of the bright-dim ratio on temperature, leads us to conclude that the bright-dim mixing is entropic, facilitated by the small energy difference between the hex-vac and 6:6-

top configurations, measured to be 0.07 eV in the experiment. The large barrier between the states, measured to be 0.84 eV in the experiment, prevents the monolayer from reaching the ground state at low temperature.

Table III. Calculated adsorption energies for specific geometries of C_{60} on Ag(111). The energy ranges given correspond to the extra Ag atoms from the vacancies being located on the surface between C_{60} molecules (low number) or in a bulk site (high number).

1-C_{60}	**E_{ads} (eV)**	**2-C_{60} configuration**	**E_{ads} (eV)**
Hex-vac	1.44 – 1.74	Hex-vac + hex-vac	1.44 – 1.74
Hex-top	1.20	Hex-vac + hex-top	1.36 – 1.51
6:6-top	1.27	Hex-vac + 6:6-top	1.40 – 1.55
6:6-vac	0.94 – 1.24	Hex-vac + 6:6-vac	1.22 – 1.52

The new DFT calculations also indicate that there is a slight (< 0.05 eV) dependence of the adsorption energy on the azimuthal orientation of the 6:6-top molecules relative to the substrate, with the most favorable positions having the C_{60} mirror planes aligned along the 30° direction, as found in STM [18] and shown in **Figure 1a**. This dependence is maintained in the 2-C_{60} configuration, one indication of a very weak anisotropic C_{60}-C_{60} interaction. On thicker films, it is known that a 4-sublattice C_{60} structure forms at low temperature as a result of anisotropic C_{60}-C_{60} interactions [32]. For our system, it appears that the orientational ordering is dominated by the C_{60}-substrate interaction rather than the anisotropic C_{60}-C_{60} interaction. This is supported by the observation that the 6:6 bond directions for this structure on Au(111) are 30° different from those on Ag(111) [4], and it also concurs with our related DFT calculations for both systems (Au(111) results are not presented here).

In conclusion, we have measured the equilibrium configuration of C_{60} molecules in the Ag(111)-(2√3x2√3)-R30° phase to determine that the two molecular states have very similar energies with a relatively large barrier between them. We have determined the geometries of the two states to be hex-vac, which consists of a C_{60} with a hexagon down on a vacancy site, and 6:6-top, which consists of a C_{60} with a 6:6 bond down on a top site. At finite temperatures, there is an entropic

distribution of the two states, with the proportion of hex-vac molecules increasing as the temperature is lowered. The flips from one state to another are spatially and temporally correlated, indicating that the flipping involves the diffusion of surface vacancies, which diffuse rapidly but are strongly attracted to C_{60} molecules.

A very similar mixed phase with flipping behavior has been observed on Au(111) [4, 16, 19], where the flipping rate was measured to be about 1 x 10^{-4} flips/s at 295 K [19]. This is a factor of ~3 lower than the results presented here for Ag(111) at the same temperature. If we assume that the pre-exponential factor is the same for Ag and Au, then we find that the energy barrier for Au is about 0.03 eV larger for Au than for Ag, or about 0.87 eV. This is consistent with the larger vacancy formation energy for Au(111) compared to Ag(111), 0.83 eV vs. 0.76 eV. For the studies of these two systems, it is fortuitous that the range where the dynamics are easily measured happens to be near room temperature for both. One difference, however, is that the correlated flipping on Au(111) is apparently not as confined to nearest neighbors [19], which may be related to differences in vacancy diffusion, or in the "attraction" of the vacancies to the C_{60} molecules. It would be interesting to explore C_{60} or similar molecules on surfaces with range of vacancy formation energies, perhaps with simulations, to gain insight into the interplay of the various interactions that affect this behavior.

We thank L. W. Bruch and V. H. Crespi for discussions of thermodynamics, and S. E. Rauterkus for assistance with the data. This work was supported by NSF Grant No. DMR-0505160, the CNRS for the INCAS project (PICS05892), the Academy of Finland, and the CSC - IT Center for Science Ltd. The DFT was supported by D. D. Johnson and the U.S. Department of Energy, Office of Basic Energy Sciences, mostly under contract DE-FG02-03ER15476 at Ames Laboratory. Ames Laboratory is operated for the U.S. DOE by Iowa State University under contract DE-AC02-07CH11358.

References

1. G. Cuniberti, K. Richter and G. Fagas, in *Lecture Notes in Physics* (Springer, Berlin, 2005), Vol. 680.
2. N. Néel, J. Kröger, L. Limot and R. Berndt, Nano Letters 8, 1291 (2008).
3. N. Néel, L. Limot, J. Kröger and R. Berndt, Phys. Rev. B 77, 125431 (2008).
4. G. Schull, N. Néel, M. Becker, J. Kröger and R. Berndt, New J. Phys. 10, 065012 (2008).
5. S. K. Yee, J. A. Malen, A. Majumdar and R. A. Segalman, Nano Letters 11, 4089 (2011).
6. J. A. Larsson, S. D. Elliott, J. C. Greer, J. Repp, G. Meyer and R. Allenspach, Phys. Rev. B 77, 115434 (2008).
7. C. Rogero, J. I. Pascual, J. Gomez-Herrero and A. M. Baro, J. Chem. Phys. 116 (2), 832 (2002).
8. J. Paloheimo, H. Isotalo, J. Kastner and H. Kuzmany, Synth. Met. 56, 3185 (1993).
9. R. Felici, M. Pedio, F. Borgatti, S. Iannotta, M. Capozi, G. Ciullo and A. Stierle, Nat Mater 4, 688 (2005).
10. W. W. Pai, H. T. Jeng, C. M. Cheng, C. H. Lin, X. Xiao, A. Zhao, X. Zhang, G. Xu, X. Q. Shi, M. A. Van Hove, C. S. Hsue and K. D. Tsuei, Phys. Rev. Lett. 104 (3), 036103 (2010).
11. X. Zhang, W. He, A. Zhao, H. Li, L. Chen, W. W. Pai, J. Hou, M. M. T. Loy, J. Yang and X. Xiao, Phys. Rev. B 75, 235444 (2007).
12. L. Tang, X. Zhang, Q. Guo, Y. N. Wu, L. L. Wang and H. P. Cheng, Phys. Rev. B 82, 125414 (2010).
13. X. D. Wang, S. Yamazaki, J. L. Li, T. Hashizume, H. Shinohara and T. Sakurai, Scanning Microscopy 8 (4), 987 (1994).
14. X. Zhang, F. Yin, R. E. Palmer and Q. Guo, Surf. Sci. 602, 885 (2008).
15. K. J. Franke, G. Schulze, N. Henningsen, J. I. Pascual, S. Zarwell, K. Rück-Braun, M. Cobian and N. Lorente, Phys. Rev. Lett. 100, 036807 (2008).
16. E. I. Altman and R. J. Colton, Phys. Rev. B 48 (24), 18244 (1993).
17. E. I. Altman and R. J. Colton, Surf. Sci. 295, 13 (1993).
18. W. Chen, H. D. Zhang, H. Huang, L. Chen and A. T. S. Wee, ACS Nano 2, 693 (2008).
19. J. A. Gardener, G. A. D. Briggs and M. R. Castell, Phys. Rev. B 80, 235434 (2009).
20. L. Tang, Z. Yangchun and Q. Guo, J. Chem. Phys. 135, 114702 (2011).

21. C. L. Hsu and W. W. Pai, Phys. Rev. B 68, 245414 (2003).
22. C. D. Liu, Z. H. Qin, J. A. Chen, Q. Guo, Y. H. Yu and G. Y. Cao, J. Chem. Phys. 134, 044707 (2011).
23. X. Q. Shi, A. B. Pang, K. L. Man, R. Q. Zhang, C. Minot, M. S. Altman and M. A. Van Hove, Phys. Rev. B 84 (23), 235406 (2011).
24. X. Q. Shi, M. A. Van Hove and R. Q. Zhang, Phys. Rev. B 85, 075421 (2012).
25. P. Wang, H. J. Zhang, Y. J. Li, C. Q. Sheng, Y. Shen, H. Y. Li, S. N. Bao and H. N. Li, Phys. Rev. B 85, 205445 (2012).
26. H. I. Li, K. Pussi, K. J. Hanna, L. L. Wang, D. D. Johnson, H. P. Cheng, H. Shin, S. Curtarolo, W. Moritz, J. A. Smerdon, R. McGrath and R. D. Diehl, Phys. Rev. Lett. 103, 056101 (2009).
27. EPAPS materials with this paper (2012).
28. J. B. Pendry, J. Phys. C: Solid State 13, 937 (1980).
29. M. I. Haftel, Phys. Rev. B 64, 125415 (2001).
30. L. W. Bruch, R. D. Diehl and J. A. Venables, Rev. Mod. Phys. 79, 1381 (2007).
31. L. L. Wang and H. P. Cheng, Phys. Rev. B 69, 165417 (2004).
32. H. Wang, C. Zeng, B. Wang, J. G. Hou, Q. Li and J. Yang, Phys. Rev. B 63, 085417 (2001).